ORIGINAL ARTICLE

Precision and Future Medicine 2023;7(1):44-54
https://doi.org/10.23838/pfm.2022.00135
pISSN: 2508-7940 · eISSN: 2508-7959

PRECISION AND FUTURE MEDICINE

# Angiogenesis effect of udenafil in a caveolin-1 deficient moyamoya disease model

## A pre-clinical animal study

Dong Hee Kim[1,2], Jeong Pyo Son[1,3], Yeon Hee Cho[1], Eun Hee Kim[1,4], Gyeong Joon Moon[5], Oh Young Bang[1,4,6]

[1]Translational and Stem Cell Research Laboratory on Stroke, Samsung Medical Center, Seoul, Korea
[2]CellnLife Inc., Seoul, Korea
[3]Advanced Radiation Technology Institute, Jeongeup Campus of Korea Atomic Energy Research Institute (KAERI), Jeongeup, Korea
[4]Stem Cell and Regenerative Medicine Institute, Samsung Medical Center, Sungkyunkwan University School of Medicine, Seoul, Korea
[5]Center for Cell Therapy, Asan Institute for Life Science, Asan Medical Center, Seoul, Korea
[6]Department of Neurology, Samsung Medical Center, Sungkyunkwan University School of Medicine, Seoul, Korea

Received: November 21, 2022
Revised: March 9, 2023
Accepted: March 14, 2023

Corresponding author:
Oh Young Bang
Department of Neurology, Samsung Medical Center, Sungkyunkwan University School of Medicine, 81 Irwon-ro, Gangnam-gu, Seoul 06351, Korea
Tel: +82-2-3410-3599
E-mail: ohyoung.bang@samsung.com



## ABSTRACT

**Purpose:** Although pathogenic mechanisms of moyamoya disease (MMD) remain unknown, recent studies suggest that it is a caveolae disease. This study evaluated the effect of udenafil, a phosphodiesterase-5 inhibitor, on angiogenesis in *in vitro* and *in vivo* MMD models.

**Methods:** Angiogenesis and vessel maturation were assessed in *in vitro* models, caveolin-1 (Cav-1) knockdown human umbilical vessel endothelial cells (HUVECs) and coronary artery smooth muscle cells (CASMCs), and in *in vivo* model of bilateral internal carotid artery occlusion (bICAo). Udenafil was administered (1,3,10, and 30 μM) in cell culture conditions, and functional studies (migration and tube formation assay) were performed and vessel maturation factors and cyclic guanosine monophosphate (cGMP) accumulation were measured.

**Results:** Udenafil (3 and 10 mg/kg) was orally administered once daily for 4 weeks in bICAo rat model, and histological analysis for angiogenesis and vessel maturation was performed. Udenafil increased vessel formation in both Cav-1 knockdown HUVEC and bICAo models without increased migration/proliferation of HUVECs and CASMCs. Udenafil increased CD31+ vessel density and NG2/Col4+ mural cell density in bICAo models. Cav-1 knockdown inhibited accumulation of cGMP, and udenafil treatment restored cGMP levels in Cav-1 knockdown HUVEC models. Vessel maturation factors (angiopoietin-1 and platelet-derived growth factor receptor-β) and angiogenic factors (endothelial nitric oxide synthase) were increased after treatment with udenafil *in vitro*.

**Conclusion:** Our results indicate that udenafil reversed cellular levels of cGMP related to Cav-1 deficiency and induced angiogenesis and vessel maturation. Further studies are warranted to confirm the therapeutic effects of this strategy in MMD.

**Keywords:** Angiogenesis; Caveolin 1; Moyamoya disease; Phosphodiesterase 5 inhibitors; Stroke

## INTRODUCTION

Moyamoya disease (MMD) is an uncommon cerebrovascular disease by internal carotid artery (ICA) stenosis leading to the development of abnormal capillary at the basement of the brain [1]. Global recognition of MMD has recently increased [2]. Although the pathogenetic mechanism of MMD vessel development remain unknown, there is growing evidence that MMD is primarily a proliferative disease (vascular cell proliferation/migration leading to luminal occlusion) characterized by aberrant angiogenesis (i.e., moyamoya vessels and thinly medial wall) [3]. We reported that caveolin-1 (Cav-1) expression were lower in MMD patients, correlating with the pathological arterial negative remodeling seen in high-resolution magnetic resonance imaging, suggesting that MMD is a caveolae disease [3,4]. In addition, lower Cav-1 expression in cellular level caused apoptosis of vascular cells and impaired angiogenesis [4].

Bypass surgery to restore cerebrovascular perfusion are the mainstay of MMD therapy, but these pose the risk of complications, such as perioperative stroke and cerebral hyper-perfusion syndrome [5]. There are no current treatments to halt progressive stenosis in MMD [5]. Medical treatment strategies for the prevention of stroke, including antiplatelet agents and statins, are of unproven benefit in MMD.

In the present study, we hypothesized that udenafil, a phosphodiesterase type-5 (PDE5) inhibitor, may be a potential therapeutic agent for increasing physiological (non-aberrant) angiogenesis in MMD models. To this end, we performed angiogenesis and migration assays, established a mechanistic basis of udenafil in *in vitro* experimental Cav-1 knockdown MMD models, and assessed *in vivo* therapeutic angiogenesis in bilateral internal carotid artery occlusion (bICAo) rat models.

## METHODS

### HUVEC and CASMC cultures

Human umbilical vessel endothelial cells (HUVECs), coronary artery smooth muscle cells (CASMCs), and all cell culture media (EGM-2 BulletKit and SmGm-2 BulletKit) were purchased from Lonza. HUVECs were cultured in EGM-2 complete media and CASMCs were cultured in SmGM-2 complete media. Both cell cultures were maintained at 37 °C in 5% $CO_2$ conditions.

### Migration assays in HUVEC and CASMC cultures

Twenty-four hours after small interfering RNA (siRNA) transfection, passage three HUVECs and passage five CASMCs were detached and re-suspended. HUVECs ($1.8 \times 10^5$ cells/well) and CASMCs ($8 \times 10^4$ cells/well) were seeded in 12 well plates and incubated at 37 °C in 5% $CO_2$. After 16 hours, wounding was simulated by scratching the cell layer using a pipette tip, and the ablated cells were washed away with phosphate buffered saline (PBS). Next, cells were cultured in complete media containing udenafil (1 and 10 μM; Dong-A ST) or blank media. Cells were left to migrate toward the wounded area for 8 or 12 hours. Images for analysis were captured using bright field microscopy at 0, 8, and 12 hours. Migration fields in the images were analyzed using ImageJ software (National Institutes of Health).

### HUVEC tube formation assay

Tube formation assays were performed using μ-slide angiogenesis (ibidi). In total, 10 μL of chilled Matrigel (BD Bioscience) was added to pre-cooled μ-slide wells and solidify for 1 hour at 37 °C. Passage three HUVECs were detached using TrypLE Express Enzyme (Gibco) and re-suspended in M199 media supplemented with fetal bovine serum (1%) and heparin (5 U/mL). The udenafil concentrations selected were 1, 3, 10, 30 μM, plus a blank. Cells ($1 \times 10^4$ cells/well) were seeded onto the Matrigel in μ-slide wells and incubated at 37 °C in 5% $CO_2$. Four hours later, images were captured using a light microscope at a magnification of 40 ×. The number of branches and loops in the captured images were calculated using ImageJ software.

### Animal surgery and udenafil treatment

Wistar-Kyoto rats were purchased from Central Lab Animal Inc. Total 47 animals were sacrificed in this study. Animals were housed in cages controlled for humidity (55% ± 5%) and temperature (22 ± 1 °C) with light/dark (12/12) cycles. Animals were subjected to surgery and monitored according to the guidelines of the Laboratory Animals Research Center (LARC; The Association for Assessment and Accreditation of the Laboratory Animal Care International [AAALAC]-approved facility) at the Samsung Medical Center. A 5% isoflurane was used for anesthesia induction, and it was maintained with 2% isoflurane in $N_2O$ and $O_2$ (7:3). Homeothermic blanket system (Harvard Apparatus) was used to monitor body temperature and maintain at 37 °C during surgery. Rats were placed in a stereotaxic frame (KOPF). A head midline incision was made using a scalpel. The periosteum was carefully removed, and the skull was exposed. High-resolution cerebral blood flow (CBF) images were taken using the Laser Doppler Imaging system (MoorLDI2-HR, Moore Instruments Inc.). Next, the

right common carotid artery, external carotid artery, ICA were exposed through a neck midline incision. The proximal and distal ICA (distance: 1 mm) was tightly double-ligated using 6–0 silk sutures, and 10 minutes later, the left ICA was occluded in the same manner. Thirty minutes later, CBF was scanned, and incisions were sutured with 5–0 monofilament sutures. Sham control groups (n=4) were operated on using only the scalp incision procedure. CBF images were acquired at 1 day after surgery. To reduce animal and surgical variation, we selected animals with a 1-day CBF of 50% or less (Supplementary Fig. 1A).

Udenafil treatment was performed following the general method reported in prior studies [6]. For oral administration, udenafil was dissolved in a Titrisol buffer (Merck). Udenafil was concentrated at 3 mg/kg/3 mL (n=10) and 10 mg/kg/3 mL (n=10) in Titrisol buffer solutions. Vehicle control (n=10) was administered as Titrisol buffer only. Udenafil was administered orally once daily for 28 days. There was no significant difference in body weight among the administration groups (Supplementary Fig. 1B).

## Tissue sample preparation

Rats were perfused transcardially with 200 mL PBS, followed by 4% paraformaldehyde (PFA) in PBS under pressure control fluid delivery at 85 mm Hg using a peristaltic pump. Rat brains were post-fixed in 4% PFA for 24 hours at 4 °C, followed by cryo-protection in 30% sucrose in PBS until they absolutely sank at 4 °C. Coronal sections (12 μm) were taken from a 1.5 to –0.5 mm area around the bregma using a cryostat, and sections were mounted onto gelatin-coated slides and dehydrated at room temperature for 30 minutes. Slides were then stored at –20 °C.

## Immunofluorescence

For immunofluorescence staining, slide sections were first incubated in 4% PFA for 30 minutes at room temperature. To retrieve antigens, sections were incubated in sodium citrate buffer (10 mM, 0.05% tween-20, pH 6.0) at 90 °C for 20 min-

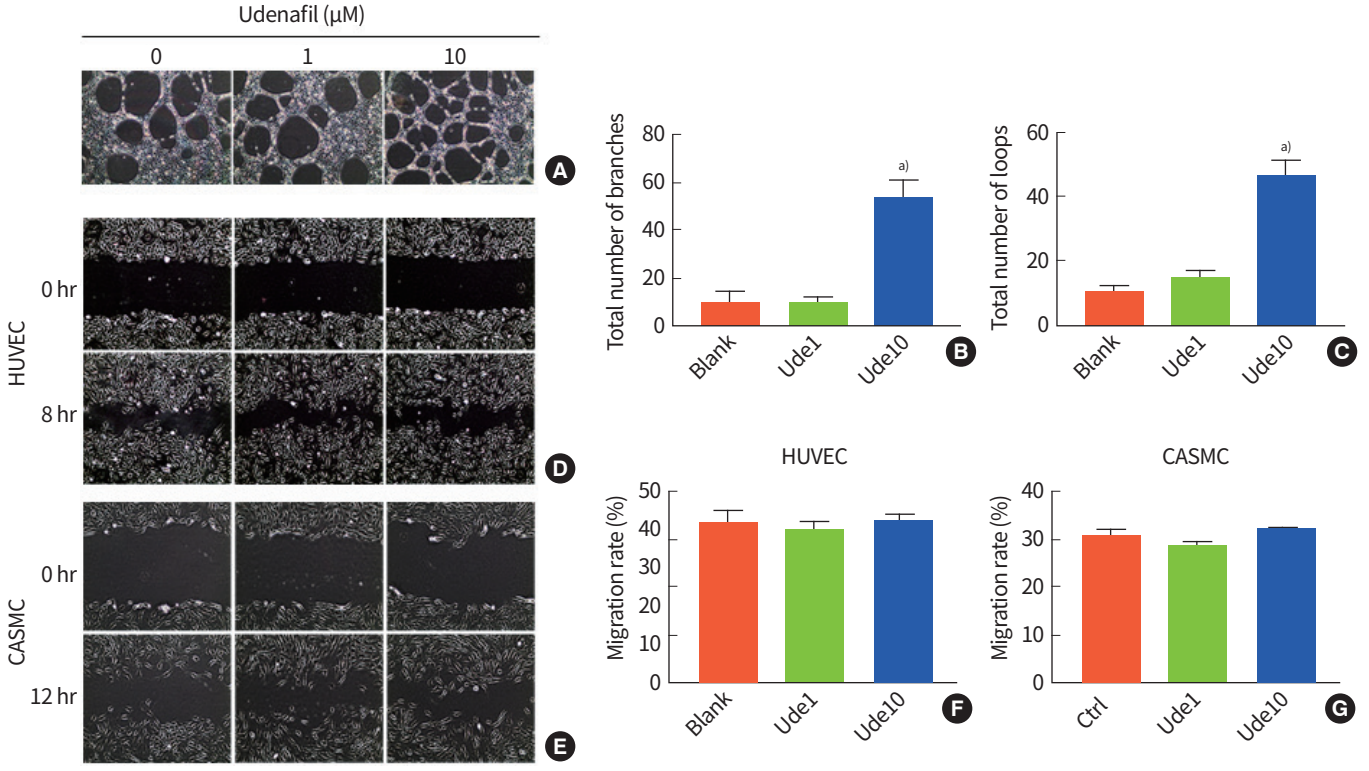


Fig. 1. *In vitro* studies for angiogenesis and migration/proliferation of human umbilical vessel endothelial cells (HUVECs) and coronary artery smooth muscle cells (CASMCs). (A) Representative images of HUVEC tube formation assay. Tube formation assay was performed to evaluate the angiogenic ability of udenafil. Images were captured at 4 hours after the assay. (B, C) Histograms of total numbers of branches and loops. Representative images of migration assay in (D) HUVECs and (E) CASMCs. Migration assay was performed to evaluate migration capability upon treatment with 1 and 10 μM udenafil. The width of the scratches was measured at 0 and 8 hours (HUVECs) or at 12 hours (CASMCs) of culture. (F, G) Histograms of relative migration values in each group. Values are presented as mean±standard error of the mean. Ctrl, control.
[a]P<0.001 compared to blank.

utes and cooled at room temperature for 20 minutes. Sections were then incubated in 0.25% triton X-100 in PBS for 15 minutes to enhance permeability. For blocking non-specific binding of antibodies, the sections were incubated in 10% horse serum and 0.25% triton X-100 in PBS for 40 minutes at room temperature. Sections were then incubated overnight at 4 °C with primary antibodies diluted in blocking solution. The following primary antibodies were used: mouse anti-CD31 conjugated Alexa fluor-488 (NOVUS Biologicals), rabbit anti-Collagen IV (Col4, Antibodies Online), and mouse anti-neuron/glia antigen 2 (NG2, Santa Cruz). After rinsing in PBS containing 0.1% tween-20 (PBST), sections were incubated with secondary antibodies for 2 hours at room temperature. The following secondary antibodies were used: Dylight 594 goat anti-rabbit immunoglobulin G (IgG, 1:200, Abcam) and Dylight 488 donkey anti-mouse IgG (1:200, Abcam). The sections were thoroughly washed in PBST three times for 10 minutes each. Finally, sections were mounted using vectashield with 4′,6-diamidino-2-phenylindole (DAPI, Vector Laboratories).

Color-merged images and single-colored images were taken from immunofluorescence slides by an EVOS microscope. Each fluorescence image was analyzed in three microscopic fields by NIH ImageJ software. CD31- and Col4- immunoreactivity was measured based on fluorescence intensity from the cerebral cortex or striatum. NG2/Col4 double-positive cells were counted from the cerebral cortex.

### Cav-1 siRNA transfection

SiRNA targeting Cav-1 3'untranslated region (UTR) and control siRNA were synthesized by Bioneer Corporation. The siRNA sequences were as follows: (1) Cav-1 siRNA, sense: 5'-GAGUCUGGUGAAGCUCACU-3', antisense: 5'-AGUGAGCUUCACCAGACUC-3'; (2) control siRNA, sense: 5'-AAUUCUCCGAACGUGUCACGU-3', antisense: 5'-ACGUGACACGUUCGGAGAAUU-3.' siRNA transfections into HUVECs and CAMSCs were performed with lipofectamine 2000 (Invitrogen) according to manufacturer's protocol. HUVECs at passage 3 were seeded with a density of 800,000 cells in a gelatin-coated 60-mm dish, and CASMCs at passage 5 were seeded with a density of 300,000 cells in a 60-mm dish. After 24 hours, cells were transfected with siRNA (50 nM) using lipofectamine 2000 (15 μL/dish) in Opti-MEM. Six hours later, media were changed with each complete growth medium.

### Western blot analysis

Cell lysates were harvested in radioimmunoprecipitation assay (RIPA) buffer (contained with a protease inhibitor cocktail), and centrifuged at 13,200 rpm for 15 minutes. Loading buffer was added to the protein sample, denatured at 100 °C for 10 minutes, and then cooled at ice. Total protein samples (20 μg) were loaded on an sodium dodecyl-sulfate polyacrylamide gel electrophoresis (SDS-PAGE) gel, and electrophoresis was performed. The separated proteins were transferred to a nitrocellulose membrane (pore size, 0.45 μm). Membranes were blocked with 5% non-fat milk and incubated with the primary antibody in blocking solution at 4 °C overnight. Next, membranes were incubated with the secondary antibody for 2 hours at room temperature. The following primary antibodies were used: mouse monoclonal glyceraldehyde-3-phosphate dehydrogenase (GAPDH) antibody (1:5,000, Santa Cruz), mouse monoclonal Cav-1 antibody (1:1,000, Invitrogen), rabbit polyclonal endothelial nitric oxide synthase (eNOS) antibody (1:1,000, Cell Signaling), rabbit polyclonal PDBF-BB antibody (1:1,000, LifeSpan BioSciences), rabbit polyclonal angiopoietin-1 (ANGPT1) antibody (1:1,000, Abcam), and rabbit monoclonal platelet-derived growth factor receptor β (PDGFRβ) antibody (1:1,000, Cell Signaling). The following secondary antibodies were used: anti-rabbit IgG horseradish peroxidase (HRP)-linked antibody (1:1,000, Cell Signaling) and anti-mouse IgG HRP-linked antibody (1:1,000, Cell Signaling).

### Cyclic guanosine monophosphate enzyme-linked immunosorbent assay

Cellular cyclic guanosine monophosphate (cGMP) levels were quantified using a cGMP enzyme-linked immunosorbent assay (ELISA) kit (Cayman Chemical). ELISA was performed according to the manufacturer's instructions. In this study, we used S-nitrosoglutathione (GSNO) as a nitric oxide (NO) donor to increase cGMP basal levels because our preliminary ELISA study showed that cGMP was not detected in lysed cells by ELISA as basal levels were too low (data not shown). The optimal dose of GSNO was determined to be 10 μM (Supplementary Fig. 2). One day after transfection, passage four HUVECs and passage six CASMCs were seeded in individual complete media containing 10 μM GSNO (NO donor, Sigma Aldrich) in 100 mm dishes. Udenafil (final concentration: 3 or 10 μM) was added to both cells at 24 hours after seeding. After 24 hours, cells were scraped using 0.1 M hydrochloric acid. Samples were centrifuged at 1,000 × g for 10 minutes. Supernatants were acetylated using 4 M potassium hydroxide and acetic anhydride. Only final samples were used in the assay. All samples were run ELISA in duplicates. Absorbance values were calcu-

lated based on the standard curve. ELISA plates were read using a SpectraMax Microplate Reader and analyzed using the SoftMax Pro Data Analysis Software (Molecular Devices).

## Statistical analysis

All error bars in graphs show mean ± standard error of the mean. One-way analysis of variance (ANOVA) analysis was followed by the Tukey honestly significant difference (HSD) *post*

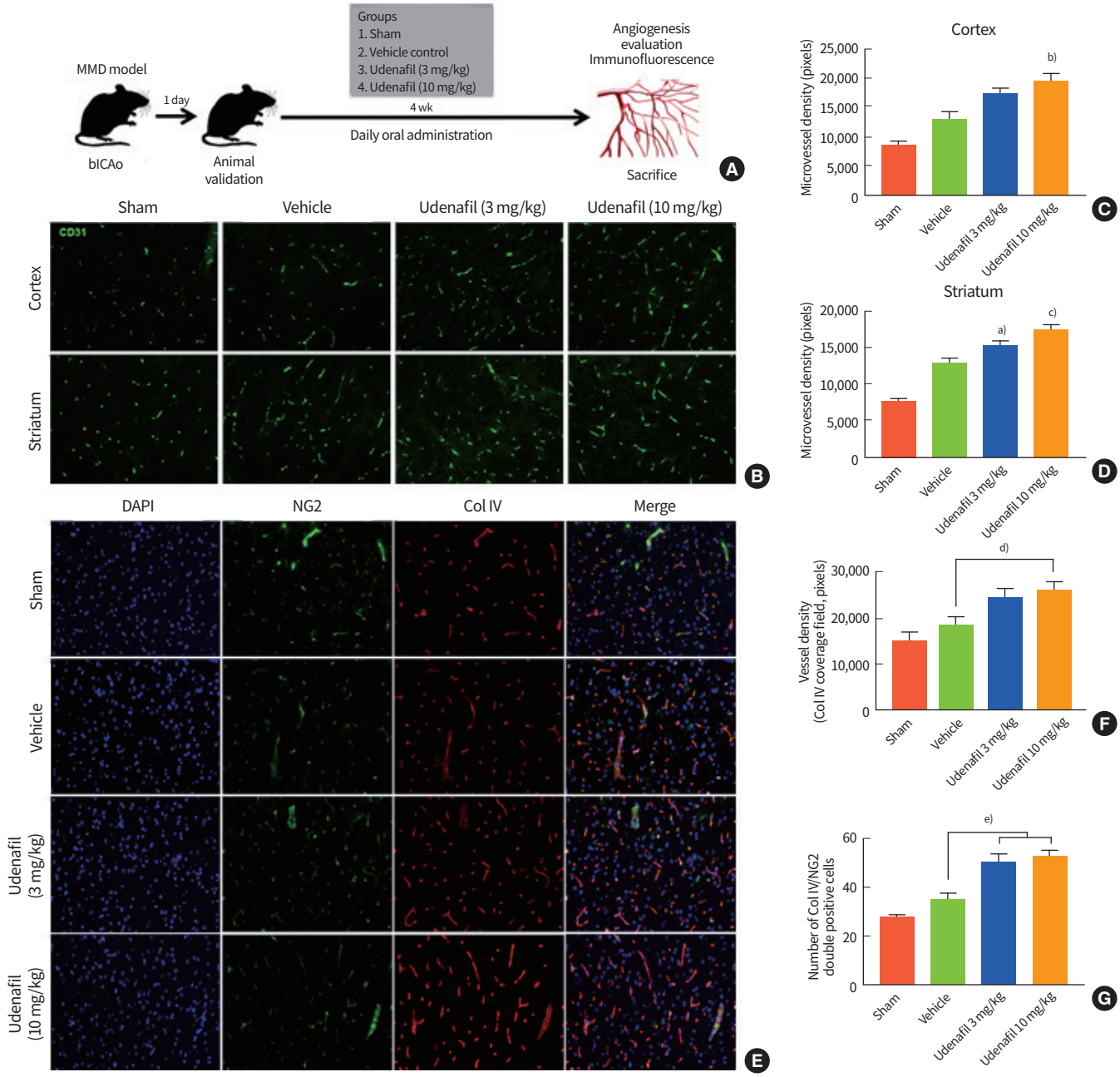


Fig. 2. *In vivo* study of angiogenesis and vessel maturation in a bilateral internal carotid artery occlusion (bICAo) model. (A) Udenafil (3 and 10 mg/kg) was orally administered daily for 4 weeks after bICAo. At 4 weeks, animals were sacrificed to evaluate angiogenesis. (B) Representative images of CD31 immunofluorescence in the cortex (top row) and striatum regions (bottom row). Daily oral treatment with udenafil (10 mg/kg) after bICAo increased microvessel density in the (C) cortex and (D) striatum. (E) Representative images of double-immunofluorescence (neuron/glia antigen 2 [NG2]/4′,6-diamidino-2-phenylindole [DAPI]) in the cortex region. (F) Collagen IV immunoreactive field (red fluorescence) represents endothelial basal membrane and vascular density. (G) NG2 positive cells indicate pericytes, and NG2/Col IV double-positive cells indicate mature vessels and vascular stability. Values are presented as mean±standard error of the mean. MMD, moyamoya disease. [a]P< 0.05; [b]P<0.01; [c]P<0.001 compared to vehicle group; [d]P<0.05; [e]P<0.01.

*hoc* test using SPSS version 20 software (IBM Co.).

## RESULTS

### Udenafil increased angiogenesis without migration/proliferation *in vitro*

To evaluate the role of udenafil on angiogenesis *in vivo*, tube formation and migration assays were performed with doses of udenafil (1 and 10 μM) under normal cell conditions. The HUVEC tube formation assay showed that 10 μM udenafil significantly increased the number of branches ($F=25.879$, $P<0.000$) and loops ($F=37.640$, $P<0.000$) compared with blank and 1 μM udenafil treatment (Fig. 1A-C). In addition, the migration assay was performed to determine whether udenafil induced migration/proliferation of HUVECs and CASMCs. Quantitative analysis showed that udenafil treatment did not change migration activity in either cell type (Fig. 1D-G).

### Udenafil enhanced angiogenesis with vessel maturation *in vivo*

To evaluate the effect of udenafil on *in vivo* angiogenesis, an animal study using bICAo was performed. Udenafil was daily administered orally from day 1 to 4 weeks, and animals were divided into two treatment groups based on the dose: 3 and 10 mg/kg (Fig. 2A). Angiogenesis was measured by CD31 immunofluorescence after udenafil treatment. Quantification results showed that 10 mg/kg udenafil treatment greatly increased microvessel density as compared with the vehicle

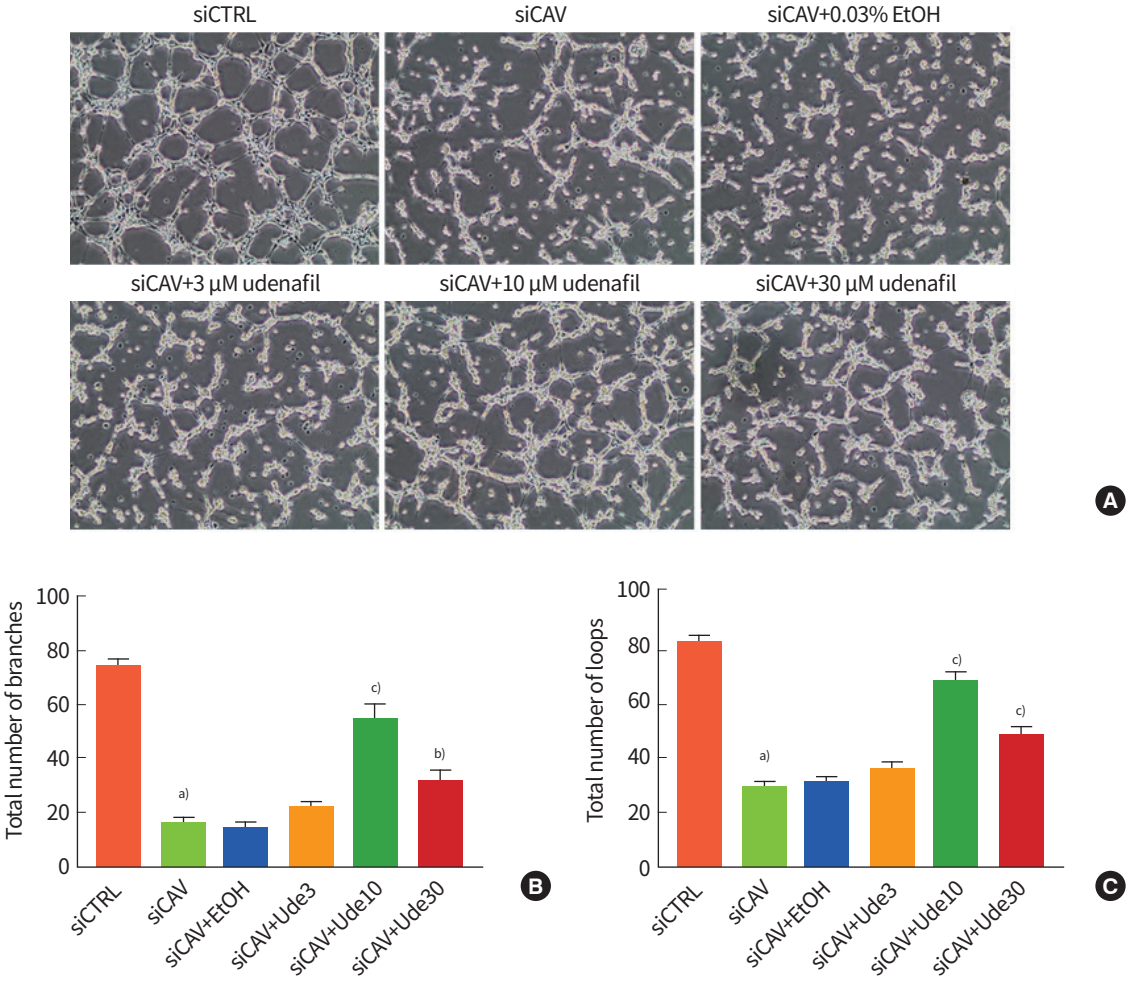


Fig. 3. *In vitro* angiogenesis assay after udenafil treatment in caveolin-1 (Cav-1) knockdown human umbilical vessel endothelial cells (HUVECs). (A) Representative images of tube formation assay. Udenafil was administered in doses of 3, 10, and 30 μM. (B, C) Histograms of total numbers of branches and loops. The ethyl alcohol (EtOH) treatment group was included in this study to rule out the effect of the solvent, because EtOH was used as a solvent for the udenafil stock. Values are presented as mean±standard error of the mean. [a]P<0.001 compared to control siRNA (siCTRL); [b]P<0.01 and [c]P<0.001 compared to Cav-1 siRNA (siCAV).

control in both the cortex (F=11.156, P=0.002) and striatum (F=28.061, P=0.000) regions. Udenafil treatment at dosages over 3 mg/kg significantly increased microvessel density in the striatum (F=28.061, P=0.034) (Fig. 2B-D). Additionally, vessel maturation was measured (Fig. 2E-G). Col4 (a marker for the endothelial basement membrane) positive signaling was analyzed as indicator of vascular density (Fig. 2F) and vessel maturation was quantified by counting Col4/NG2 (a marker for pericytes) double-positive cells (Fig. 2G) in the cortex region. Col4/NG2 double-positive cells were significantly higher in the udenafil treatment group than in the vehicle group (F=11.398, P=0.006 vs. 3 mg/kg and P=0.001 vs. 10 mg/kg udenafil group).

### Udenafil restored angiogenesis in Cav-1 knockdown *in vitro* models

We performed transient Cav-1 downregulation using siRNA transfection in HUVECs and performed the tube formation assay with udenafil treatment. Transfection with Cav-1 siRNA inhibited target gene expression , and udenafil did not influence levels of Cav-1 expression (Supplementary Fig. 3). In this experiment, the range of udenafil dose was increased to identify the most optimal concentration (3, 10, and 30 μM). Cav-1 siRNA (siCAV-1) transfection inhibited angiogenic ability, and udenafil treatment restored that (Fig. 3A). Quantitative analysis showed that siCav-1 transfection completely suppressed the formation of branches (F=63.327, P=0.000) and loops (F=88.198, P=0.000), and 10 and 30 μM udenafil doses significantly increased tube branches (P=0.000 vs. 10 μM and P=0.007 vs. 30 μM udenafil) (Fig. 3B) and loops (P=0.000 vs. both 10 and 30 μM udenafil) (Fig. 3C) compared with siCav-1 transfection only. Among the tested doses, 10 μM udenafil was selected as an optimal dose for further experiments.

### Cav-1 downregulated cGMP accumulation, and udenafil restored cGMP levels and induced expression of angiogenic and vessel maturation factors

In both Cav-1 knockdown HUVECs and CASMCs, udenafil treatment did not increase Cav-1 expression (Fig. 4A, B). However, ELISA tests for cGMP showed that Cav-1 knockdown reduced cGMP concentrations in both cell types (HUVEC, F=8.969, P=0.005; CASMC, F=4.289, P=0.032) and cGMP levels significantly increased with 10 μM udenafil treatment in Cav-1 knockdown HUVECs (P=0.048) (Fig. 4C, D). Western blot analysis was performed to analyze expression levels of eNOS and platelet-derived growth factor-BB (PDGFBB) in HUVECs and ANGPT1 and PDGFRβ in CASMCs (Fig. 4I, J). Treatment with 10 μM udenafil increased eNOS expression (F=170.376, P=0.000) in HUVECs (Fig. 4E) as well as ANGPT-1 (F=5.711, P=0.014 vs. control siRNA [siCTRL]) and PDGFRβ (F=10.403, P=0.005 vs. siCAV) in CASMCs (Fig. 4F, G). PDGFBB expression in HUVECs was significantly downregulated in siCav-1 but was not significantly increased by treatment with udenafil (Fig. 4H).

## DISCUSSION

The main findings of this study were as follows: (1) udenafil (10 μM) induced tube formation without migration/proliferation of endothelial cells in Cav-1 knockdown *in vitro* models for MMD; (2) udenafil induced angiogenesis accompanied by vessel maturation in *in vivo* models of bICAo; (3) angiogenic factors, such as eNOS, ANGPT1, and PDGFRβ, increased after treatment with 10 μM udenafil; and (4) Cav-1 downregulation reduced cGMP concentration, while udenafil restored cGMP levels in HUVECs.

Although PDE5 inhibitors (including udenafil, sildenafil, tadalafil, and vardenafil) have been developed for the cure for erectile dysfunction, there has recently been immense interest in finding new clinical uses of PDE5 inhibitors for various diseases, including cardiovascular disease, diabetes, and cancer [7]. PDE5 inhibitors have been found to promote angiogenesis and functional recovery after stroke [8]. Udenafil markedly attenuates the compensatory development of right ventricular hypertrophy and reduces pulmonary artery wall thickness in monocrotaline-induced pulmonary artery hypertension (PAH) models [6]. PDE5 inhibitors are now widely used in the management of PAH [9]. The treatment options established for PAH may also be effective in MMD, because MMD and PAH share many features. First, the pathological features of PAH are similar to those of MMD, such as intimal hypertrophy, arterial remodeling, *in situ* thrombosis, and vasoconstriction [10]. Second, with regard to biochemical features, decreased serum levels of the biomarker Cav-1 have been reported in both PAH and MMD [11,12]. In addition, it has been reported that Cav-1, a scaffolding protein of the caveolae plasma membrane, is involved in the pathogenesis of cancer and vascular diseases [13]. Studies showed that Cav-1 overexpression enhanced caveolae formation and induced capillary tube formation by nearly three-fold, while Cav-1 downregulation decreased *in vitro* and *in vivo* vessel formation and was associated with pathological angiogenesis [13-15]. Another study showed that Cav-1 involved in endotherial progenitor cell recruitment from the bone marrow [16]. Last-

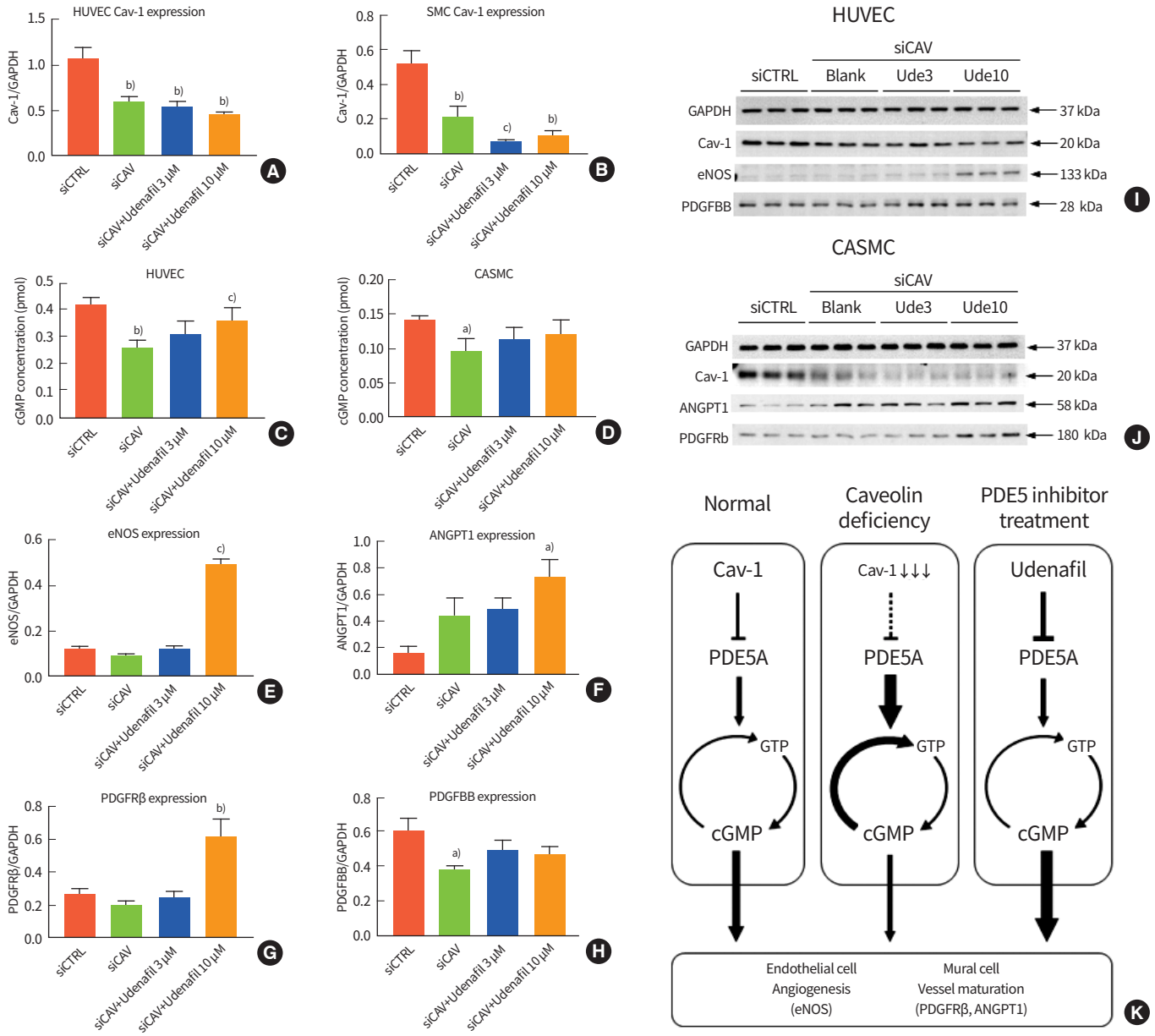


Fig. 4. Molecular change associated with angiogenesis and vessel maturation factors after udenafil treatment. Western blot analysis was performed to investigate the expression of angiogenic factors and vessel maturation factors in (I) human umbilical vessel endothelial cells (HUVECs) and (J) coronary artery smooth muscle cells (CASMCs). Histograms showing caveolin-1 (Cav-1) expression after small interfering RNA (siRNA) transfection and udenafil treatment in HUVECs (A) and CASMCs (B). Cycle guanosine monophosphate (cGMP) levels were measured after treatment with udenafil and S-nitrosoglutathione (GSNO) in Cav-1 knockdown HUVECs (C) and CASMCs (D). GSNO (10 μmol/L) basal media was used to upregulate baseline cGMP levels. Quantitative analysis of (E) endothelial nitric oxide synthase (eNOS), (F) angiopoietin-1 (ANGPT1), (G) platelet-derived growth factor receptor β (PDGFRβ), and (H) platelet-derived growth factor-BB (PDGFBB). (K) Possible underlying mechanism of udenafil treatment in moyamoya disease (MMD). In normal physiology, Cav-1 regulates phosphodiesterase type-5 (PDE5) in dependent homeostatic manner. In Cav-1 deficient conditions, such as MMD, Cav-1 downregulation consequently leads to cGMP accumulation by PDE5 activation, and PDE5 inhibitor treatment restores cGMP levels. Restored cGMP induces angiogenesis in endothelial cells and vessel maturation in mural cells. Values are presented as mean±standard error of the mean. GAPDH, glyceraldehyde-3-phosphate dehydrogenase; SMC, smooth muscel cell; GTP, guanosine triphosphate. [a]P<0.05, [b]P<0.01, and [c]P<0.001 compared to control siRNA (siCTRL); [d]P<0.05 compared to Cav-1 siRNA (siCAV).

ly, MMD and PAH share genetic similarities, namely, that homozygosity in ring finger protein 213 (*RNF213*) leads to MMD and PAH in the same patients or families [17,18].

Number of studies have reported vasodilating effects of PDE5 inhibitors. For example, PDE5 inhibitors have resulted in improved exercise capacity in PAH patients by increasing

NO levels [19]. PDE5 inhibitors block the cGMP degradation, leading to vessel relaxation due to the increase in cGMP levels. NO stimulates cytosolic guanylate cyclase and increases cGMP levels in vascular smooth muscle cells, leading to relaxation of vascular tone [20]. PDE5 inhibitors induce vasodilation via an increase in cGMP levels in pulmonary vascular smooth muscle cells [9]. However, relatively little is known about the role of PDE5 inhibitors on angiogenesis in caveolae disease.

The present study showed that udenafil enhanced angiogenic capacity in both *in vitro* and *in vivo* experiments. Our results are in line with those of previous studies showing that PDE5 inhibitors enhance angiogenesis in endothelial cells and regulate migration and proliferation of various cell types [21-23]. And PDE5 was inhibited by direct interaction with Cav-1 [24]. The present study showed that udenafil did not affect Cav-1 expression levels in vessel cells and that Cav-1 downregulation in HUVECs and CASMCs resulted in decreased cGMP levels. Such decreased cGMP levels were restored by PDE5 inhibitors in HUVECs. These findings indicate that udenafil treatment induces the accumulation of cGMP in Cav-1 deficient conditions. Thus, udenafil could be a therapeutic modality for MMD and caveolae diseases. This is the first study to show the effects of PDE5 inhibitors in a caveolae disease model.

Our present study showed that udenafil increased vessel maturation factors and induced vessel maturation without migration/proliferation of vascular cells. Pericytes are mural cells surrounding endothelial cells in the capillary and play critical roles in vessel maturation and maintenance of vascular morphogenesis [25]. PDGFBB/PDGFRβ signaling is essential for pericyte proliferation and recruitment to endothelial progenitor cells [26,27]. A variety of signaling factors, including PDGFBB/PDGFRβ and ANGPT1/Tie-2, mediate pericyte-endothelial cell interactions, resulting in vascular maturation [28]. Aberrant angiogenesis could be associated with the development of intracranial large artery stenosis and moyamoya vessels in patients with MMD. Aberrations in pericyte-endothelial cell signaling networks contribute to tumor angiogenesis [29]. Our results of molecular analysis indicate that udenafil increases expression of vessel maturation factors in mural cells. Udenafil increased eNOS expression in endothelial cells, which is associated with angiogenesis. Likewise, udenafil upregulated PDGFRβ and ANGPT1 expression in mural cells, which are associated with pericyte-endothelial cell interactions and vessel maturation. Fig. 4K summarizes the possible mechanisms of action underlying the effects of udenafil on activation of endothelial cells and mural cells for enhanced angiogenesis with appropriate vessel maturation.

Our study had limitations. In the present study, we used a bICAo model. Although bICAo is a suitable method for evaluation of therapeutic agents, this model cannot represent an MMD animal model. There is no relevant animal model for MMD, because histopathological studies of vascular wall structure in *Rnf213* -/- variants showed no apparent abnormalities in mutant mice, such as intimal hyperplasia or medial layer thinness [30]. Moreover, our *in vivo* analysis did not contain histological data of stenotic ICA portions, since we focused on therapeutic angiogenesis from udenafil treatment in the cortex region. Further studies are needed with MMD and Cav-1 knockout animal models. We are currently developing an *in vitro* endothelial and smooth muscle cell system using induced pluripotent stem cells from *RNF213* variant MMD patients.

The results of our study showed that udenafil reversed the decreased cellular cGMP levels associated with Cav-1 deficiency and induced angiogenesis and vessel maturation. These findings suggest that PDE5 inhibitors could be useful as a therapeutic agent to increase angiogenesis and vessel maturation in Cav-1 deficient conditions such as MMD. Notwithstanding the shortages of our disease model, our results provide a molecular background for the role of PDE5 inhibitors in MMD. Further studies are warranted to confirm the therapeutic effects of this strategy using animal models of MMD.

## CONFLICTS OF INTEREST

No potential conflict of interest, including CellnLife Inc., relevant to this article was reported.

## ACKNOWLEDGMENTS

This research was supported by a grant from the Bio & Medical Technology Development Program of the National Research Foundation (NRF) funded by the Korean government (MSIT) (2018M3A9H1023675).

## ORCID

Dong Hee Kim https://orcid.org/0000-0003-3719-012X
Jeong Pyo Son https://orcid.org/0000-0002-8655-3495
Yeon Hee Cho https://orcid.org/0000-0001-8856-7340
Eun Hee Kim https://orcid.org/0000-0003-1580-3204

Gyeong Joon Moon https://orcid.org/0000-0002-2851-9563
Oh Young Bang https://orcid.org/0000-0002-7962-8751

## AUTHOR CONTRIBUTIONS

Conception or design: DHK, OYB.
Acquisition, analysis, or interpretation of data: DHK, JPS, YHC.
Drafting the work or revising: DHK, EHK, GJM, OHB.
Final approval of the manuscript: OYB.

## REFERENCES

1. Kuroda S, Houkin K. Moyamoya disease: current concepts and future perspectives. Lancet Neurol 2008;7:1056-66.
2. Bang OY, Chung JW, Kim DH, Won HH, Yeon JY, Ki CS, et al. Moyamoya disease and spectrums of RNF213 vasculopathy. Transl Stroke Res 2020;11:580-9.
3. Bang OY, Fujimura M, Kim SK. The pathophysiology of moyamoya disease: an update. J Stroke 2016;18:12-20.
4. Chung JW, Kim DH, Oh MJ, Cho YH, Kim EH, Moon GJ, et al. Cav-1 (Caveolin-1) and arterial remodeling in adult moyamoya disease. Stroke 2018;49:2597-604.
5. Fujimura M, Shimizu H, Inoue T, Mugikura S, Saito A, Tominaga T. Significance of focal cerebral hyperperfusion as a cause of transient neurologic deterioration after extracranial-intracranial bypass for moyamoya disease: comparative study with non-moyamoya patients using N-isopropyl-p-[(123)I]iodoamphetamine single-photon emission computed tomography. Neurosurgery 2011;68:957-65.
6. Kang KK, Ahn GJ, Sohn YS, Ahn BO, Kim WB. DA-8159, a new PDE5 inhibitor, attenuates the development of compensatory right ventricular hypertrophy in a rat model of pulmonary hypertension. J Int Med Res 2003;31:517-28.
7. Baillie GS, Tejeda GS, Kelly MP. Therapeutic targeting of 3',5'-cyclic nucleotide phosphodiesterases: inhibition and beyond. Nat Rev Drug Discov 2019;18:770-96.
8. Olmestig JN, Marlet IR, Hainsworth AH, Kruuse C. Phosphodiesterase 5 inhibition as a therapeutic target for ischemic stroke: a systematic review of preclinical studies. Cell Signal 2017;38:39-48.
9. Clave MM, Maeda NY, Thomaz AM, Bydlowski SP, Lopes AA. Phosphodiesterase type 5 inhibitors improve microvascular dysfunction markers in pulmonary arterial hypertension associated with congenital heart disease. Congenit Heart Dis 2019;14:246-55.
10. McLaughlin VV, Shah SJ, Souza R, Humbert M. Management of pulmonary arterial hypertension. J Am Coll Cardiol 2015;65:1976-97.
11. Huang J, Wolk JH, Gewitz MH, Loyd JE, West J, Austin ED, et al. Enhanced caveolin-1 expression in smooth muscle cells: possible prelude to neointima formation. World J Cardiol 2015;7:671-84.
12. Wang KY, Lee MF, Ho HC, Liang KW, Liu CC, Tsai WJ, et al. Serum caveolin-1 as a novel biomarker in idiopathic pulmonary artery hypertension. Biomed Res Int 2015;2015:173970.
13. Frank PG, Woodman SE, Park DS, Lisanti MP. Caveolin, caveolae, and endothelial cell function. Arterioscler Thromb Vasc Biol 2003;23:1161-8.
14. Chang SH, Feng D, Nagy JA, Sciuto TE, Dvorak AM, Dvorak HF. Vascular permeability and pathological angiogenesis in caveolin-1-null mice. Am J Pathol 2009;175:1768-76.
15. Liu J, Wang XB, Park DS, Lisanti MP. Caveolin-1 expression enhances endothelial capillary tubule formation. J Biol Chem 2002;277:10661-8.
16. Sbaa E, Dewever J, Martinive P, Bouzin C, Frerart F, Balligand JL, et al. Caveolin plays a central role in endothelial progenitor cell mobilization and homing in SDF-1-driven postischemic vasculogenesis. Circ Res 2006;98:1219-27.
17. Chang SA, Song JS, Park TK, Yang JH, Kwon WC, Kim SR, et al. Nonsyndromic peripheral pulmonary artery stenosis is associated with homozygosity of RNF213 p.Arg4810Lys regardless of co-occurrence of moyamoya disease. Chest 2018;153:404-13.
18. Fukushima H, Takenouchi T, Kosaki K. Homozygosity for moyamoya disease risk allele leads to moyamoya disease with extracranial systemic and pulmonary vasculopathy. Am J Med Genet A 2016;170:2453-6.
19. Archer SL, Michelakis ED. Phosphodiesterase type 5 inhibitors for pulmonary arterial hypertension. N Engl J Med 2009;361:1864-71.
20. Corbin JD. Mechanisms of action of PDE5 inhibition in erectile dysfunction. Int J Impot Res 2004;16 Suppl 1:S4-7.
21. Adderley SP, Joshi CN, Martin DN, Tulis DA. Phosphodiesterases regulate BAY 41-2272-induced VASP phosphorylation in vascular smooth muscle cells. Front Pharmacol 2012;3:10.
22. Sahara M, Sata M, Morita T, Nakajima T, Hirata Y, Nagai R. A phosphodiesterase-5 inhibitor vardenafil enhances angiogenesis through a protein kinase G-dependent hypoxia-inducible factor-1/vascular endothelial growth factor pathway. Arterioscler Thromb Vasc Biol 2010;30:1315-24.
23. Wong JC, Fiscus RR. Essential roles of the nitric oxide (no)/cGMP/protein kinase G type-Iα (PKG-Iα) signaling path-

way and the atrial natriuretic peptide (ANP)/cGMP/PKG-Iα autocrine loop in promoting proliferation and cell survival of OP9 bone marrow stromal cells. J Cell Biochem 2011; 112:829-39.
24. Mahavadi S, Bhattacharya S, Kumar DP, Clay C, Ross G, Akbarali HI, et al. Increased PDE5 activity and decreased Rho kinase and PKC activities in colonic muscle from caveolin-1-/- mice impair the peristaltic reflex and propulsion. Am J Physiol Gastrointest Liver Physiol 2013;305: G964-74.
25. Yamazaki T, Mukouyama YS. Tissue specific origin, development, and pathological perspectives of pericytes. Front Cardiovasc Med 2018;5:78.
26. Winkler EA, Bell RD, Zlokovic BV. Pericyte-specific expression of PDGF beta receptor in mouse models with normal and deficient PDGF beta receptor signaling. Mol Neurodegener 2010;5:32.
27. Lindahl P, Johansson BR, Leveen P, Betsholtz C. Pericyte loss and microaneurysm formation in PDGF-B-deficient mice. Science 1997;277:242-5.
28. Jain RK, Booth MF. What brings pericytes to tumor vessels? J Clin Invest 2003;112:1134-6.
29. Raza A, Franklin MJ, Dudek AZ. Pericytes and vessel maturation during tumor angiogenesis and metastasis. Am J Hematol 2010;85:593-8.
30. Sonobe S, Fujimura M, Niizuma K, Nishijima Y, Ito A, Shimizu H, et al. Temporal profile of the vascular anatomy evaluated by 9.4-T magnetic resonance angiography and histopathological analysis in mice lacking RNF213: a susceptibility gene for moyamoya disease. Brain Res 2014; 1552:64-71.